Physica B 185 (1993) 264–283
North-Holland

PHYSICA B

Electrical and optical characterization of SiC

G. Pensl[1]
Institut für Angewandte Physik, Universität Erlangen–Nürnberg, Erlangen, Germany

W.J. Choyke[2]
Department of Physics and Astronomy, University of Pittsburgh, USA

We review the current use of electrical and optical methods to study the semiconducting properties of SiC. More specifically we treat Hall measurements, deep-level transient spectroscopy, infrared absorption and luminescence. Some very recent results, not yet available in the literature, on donor and acceptor levels in 3C-SiC, 4H-SiC and 6H-SiC are discussed.

Introduction

The current interest in the rapid development of SiC as a semiconductor for high-temperature, high-power, high-frequency and radiation-resistant device technology is that there is now a clearcut need for such devices in a multitude of applications. However, while the economic driving force is a necessary condition, it is not a sufficient condition for implementing such a technology in terms of modern planar device structures. The recognition that boule growth in SiC was possible (Tairov and Tsvetkov, 1978 [1]) and the implementation of CVD growth of SiC on Si in 1983 by Nishino, Powell and Will [2] has provided the foundation for our present ability to grow SiC with good enough perfection and control to develop excellent devices. In order to improve the device performance and wafer die yields, it is necessary to thoroughly characterize the starting material with respect to its electrical and optical properties as well as to establish a microscopic understanding of defects. Regarding SiC we are just beginning to solve urgent problems such as the identification of the chemical nature or atomic and electronic structure of defects.

The exciting feature of SiC is its appearance in many different polytypes providing a lone cubic (3C), a great number of hexagonal (2H, 4H, 6H, . . .) and also a great number of rhombohedral structures (15R, 21R, . . .). In this paper, our discussion is restricted to a selection of electrically active impurity centers in combination with the 3C, 4H and 6H polytypes that are important for device applications. Although the arrangement of next neighbors is the same for each Si and C atom in all polytypes, the second and third neighbor shell result in slightly altered arrangements leading to crystallographically inequivalent lattice sites (3C: one cubic (k); 4H: one cubic (k) and one hexagonal (h); 6H: two cubic (k_1, k_2) and one hexagonal (h)) [3]. It is expected that impurities substituting at inequivalent lattice sites of a particular polytype reveal differing electronic properties. In part I we report on the electrical properties and in part II on the optical properties of such centers.

Correspondence to: G. Pensl, Institut für Angewandte Physik, Universität Erlangen–Nürnberg, Staudtstrasse 7, W-8522 Erlangen, Germany.
[1] Author of part I of this article.
[2] Author of part II of this article.

1. Electrical characterization of SiC

Hall effect and deep-level transient spectroscopy (DLTS) are mainly used to determine electrical parameters of impurities or more complex centers such as concentrations, ionization energies or electrical capture cross-sections for electrons and holes. Dopants (donors or acceptors) that govern the conductivity type are investigated by Hall measurements, while levels located energetically deeper than the dopants – termed 'deep levels' – are monitored by DLTS. For a review on electrical methods, see ref. [4]. In SiC the impurities nitrogen and aluminum are the usual shallow dopants that produce n- or p-type conductivity. The doping of SiC can either occur during crystal growth or by subsequent ion implantation and annealing. Nominally undoped crystals are n-type caused by residual nitrogen.

We have performed conductivity and Hall measurements on n- and p-type SiC samples using the Van der Pauw method. The investigated 3C-SiC samples were grown by NASA-LEWIS, Cleveland, the 4H- and 6H-SiC samples were grown by Siemens AG, Erlangen. The measurements were performed in a plane perpendicular to the c-axis. Ohmic contacts were fabricated on the corners of each square sample (typical size: $5 \times 5\ \mathrm{mm}^2$) by evaporating Ti in the case of n-type and Al in the case of p-type SiC and subsequent annealing in a rapid isothermal annealing (RIA) system at 900°C for 5 min. Two different Hall set-ups were used to cover the temperature range from 30 to 800 K [5]. The low-temperature equipment (30–300 K) consists of a conventional He-flow cryostat with temperature control and He exchange gas within the sample chamber. The high-temperature chamber (300–800 K) is filled with an Ar exchange gas (1 mbar). The hot end of the sample chamber is mounted in the upright position to minimize convection close to the sample. The sample holder is designed in such a way that it can be used for both set-ups. The magnetic field applied is 0.4 T.

Ionization energies ΔE_i and concentrations N_i of the prevailing dopants, as well as the concentration of the compensation N_{comp}, are obtained from a fit of the neutrality eq. (1) to the temperature variation of the measured free-carrier concentration n or p. For n-type semiconductors, the free electron concentration is given by

$$n = \frac{r_{\mathrm{H}}(T)}{|e|\,|R_{\mathrm{H}}|}$$

where $r_{\mathrm{H}}(T)$ and R_{H} are the Hall scattering factor and the Hall coefficient, respectively. Additional information on the scattering mechanisms of free carriers and on the crystal quality can be deduced from the Hall mobility

$$\mu_{\mathrm{H}} = \sigma\,|R_{\mathrm{H}}|\,.$$

The neutrality equation of a nondegenerate, n-type semiconductor with τ different donor species can be written

$$n + N_{\mathrm{comp}} = \sum_{i=1}^{\tau} \frac{N_i}{(g_i n/N_c)\exp(\Delta E_i/kT) + 1} \qquad (1)$$

where $N_c = 2M_c(2\pi\, m^*_{\mathrm{d,e}}\, k\, T/h^2)^{3/2}$
= density of states in the conduction band,
M_c = number of equivalent conduction-band-minima,
$m^*_{\mathrm{d,e}}(T) = (m^*_{\perp,\mathrm{e}}(T)\, m^*_{\parallel,\mathrm{e}}(T))^{1/3}$
= density-of-states effective mass of the conduction band,
g_i = spin degeneracy factor,
k = Boltzmann constant.

1.1. Nitrogen donor

First we discuss Hall results of nitrogen-doped SiC samples. The parameters used for the evaluation of the Hall data are summarized in table 1. Kaplan et al. [6] and Dean et al. [7] determined the effective electron masses of the 3C polytype by cyclotron resonance and two-electron luminescence spectroscopy, while the corresponding values for the 4H and 6H polytype are obtained from the analysis of nitrogen-related IR absorption lines which are attributed to transitions from the ground state to effective-

Table 1
Parameters used for the evaluation of Hall data of n-type 3C-, 4H- and 6H-SiC polytypes.

Electron parameters	SiC polytypes 3C	4H	6H
$m^*_{\parallel,e}$ (in m_0)	0.677 [6,7]	0.22 [8]	0.34 [9]
$m^*_{\perp,e}$ (in m_0)	0.247 [6,7]	0.17 [8]	0.24 [9]
$m^*_{d,e}$ (in m_0)	0.346	0.19	0.27
M_C	3 [6,7,10]	6[a] [11,12]	6[a] [11,12]
g	2[a]	2[a]	2[a]
$r_H(T)$	1[a]	1[a]	1[a]

[a] Assumed value.

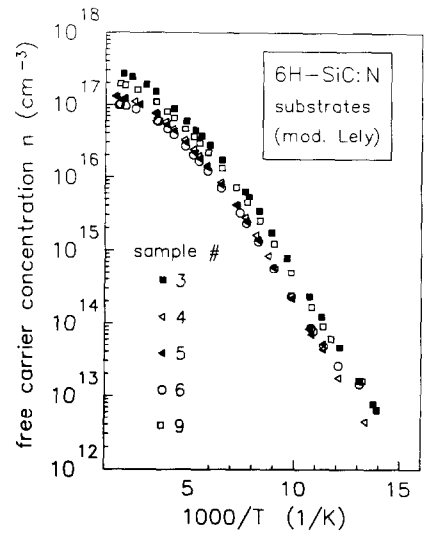

Fig. 1. Free electron concentration vs reciprocal temperature as obtained from Hall measurements of various N-doped 6H-SiC crystals. The impurity parameters are obtained from a fit of eq. (1) to the experimental Hall data.

mass-like excited states [8,9]; for details, see part II. The density-of-states effective mass of the conduction band $m^*_{d,e}$ is considered to be independent of the temperature. The number of equivalent conduction-band-minima M_c that contribute to the electron transport is expected to be 3, 6 and 6 for the 3C, 4H and 6H polytype, respectively. The Hall scattering factor $r_H(T)$ is unknown and is assumed to be 1 for all temperatures used. Because of these uncertainties, the evaluated Hall data are affected by systematic errors, which may lead to an estimated deviation of impurity concentration up to a factor of two and of impurity ionization energies up to ±10%.

Figure 1 shows the free-electron carrier concentration n as a function of the reciprocal temperature for five N-doped 6H-SiC samples. The presence of two donor levels ($\Delta E_{N,1}$, $N_{N,1}$) and ($\Delta E_{N,2}$, $N_{N,2}$) is required to fit the experimental electron concentration over the entire temperature range. The ionization energies of the donor levels are $\Delta E_{N,1} = 85.5$ meV and $\Delta E_{N,2} = 125$ meV. The ratio of the concentration of these donors $N_{N,1} : N_{N,2}$ is approximately 1:2. The absolute nitrogen concentrations are of the order of $(1\text{–}2) \times 10^{17}$ cm^{-3}; the compensation results in $N_{comp} \approx 2 \times 10^{16}$ cm^{-3}. Hexagonal (h) and cubic (k_1, k_2) lattice sites have a relative abundance of 1:2 in the 6H polytype. Assuming an equal distribution of nitrogen donors on substitutional sites, a speculative assignment can be made by identifying N-atoms on h-lattice sites with donor level 1 and nitrogen on k_1- and k_2-lattice sites with donor level 2. The two differing cubic sites (k_1, k_2) cannot be resolved in energy by the Hall analysis (for comparison with optical data, see part II). Figures 2(a) and (b) show the free electron concentration $n(1/T)$ and Hall mobility $\mu(T)$ of three high-quality 6H-SiC samples grown either by the modified Lely- [13], LPE- [14] or CVD-method [15] as indicated in the figure. The following data are obtained from the Hall analysis:

#11: $\Delta E_{N,1} = 88$ meV, $\Delta E_{N,2} = 140$ meV,
$N_{comp} = 1.5 \times 10^{16}$ cm^{-3},
$N_{N,1} = 3 \times 10^{16}$ cm^{-3},
$N_{N,2} = 6 \times 10^{16}$ cm^{-3};

#12: $\Delta E_{N,1} = 100$ meV, $\Delta E_{N,2} = 150$ meV,
$N_{comp} = 1.1 \times 10^{13}$ cm^{-3},
$N_{N,1} = 1.2 \times 10^{16}$ cm^{-3},
$N_{N,2} = 2 \times 10^{16}$ cm^{-3};

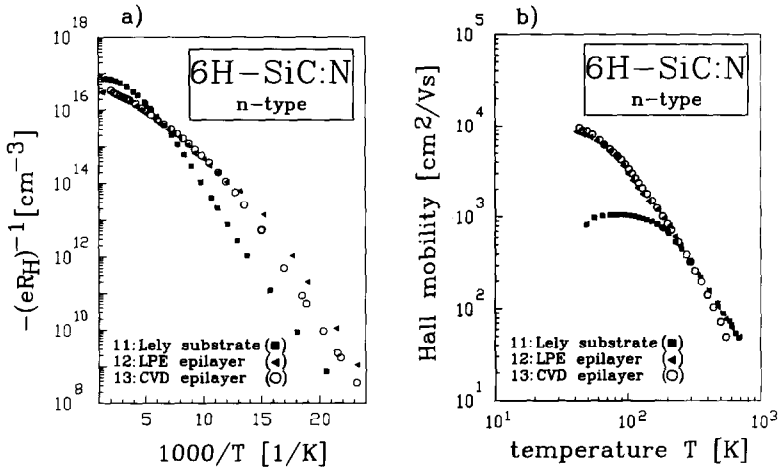

Fig. 2. Results of conductivity and Hall measurements of three N-doped 6H-SiC samples grown by different growth techniques (modified Lely method [13], liquid phase epitaxy [14], chemical vapor deposition [15]). (a) Free electron concentration $n = -1/eR_H$ as a function of the reciprocal temperature. (b) Hall mobility as a function of the temperature. The impurity parameters are given in the text.

#13: $\Delta E_{N,1} = 91\,\text{meV}$, $\Delta E_{N,2} = 145\,\text{meV}$,
$N_{comp} = 3 \times 10^{14}\,\text{cm}^{-3}$,
$N_{N,1} = 9 \times 10^{15}\,\text{cm}^{-3}$,
$N_{N,2} = 2 \times 10^{16}\,\text{cm}^{-3}$;

In the epitaxial-grown layers, the N content can be reduced to a concentration of less than $10^{15}\,\text{cm}^{-3}$; the compensation reaches values between $10^{13}\,\text{cm}^{-3}$ and a few $10^{14}\,\text{cm}^{-3}$. These low concentrations and also the crystalline perfection of the epilayers are reflected in Hall mobilities of around $10\,000\,\text{cm}^2/\text{V s}$ at low temperatures. In fig. 2(b), the maximum mobility of the Lely substrate, which contains a higher concentration of N donors and is strongly compensated, only reaches a value of $1000\,\text{cm}^2/\text{V s}$. The room temperature values are around $400\,\text{cm}^2/\text{V s}$ for all three 6H samples indicating that the ionized impurity scattering mainly limits the low-temperature tail of the $\mu(T)$ curve and its maximum value. L. Patrick [16] pointed out that the electron mobility strongly differs between the various polytypes because of the different number of conduction-band-minima lying at the Brillouin zone boundary and the differing effective masses. In the temperature range from 300 to 800 K, the electron mobility is expected to be dominated by acoustic phonon and intervalley scattering. In contrast, the hole mobility should not vary so strongly with the polytype because the valence band maximum is located at the Γ-point for each polytype. A quantitative fit of the theoretical scattering mechanisms to the experimental $\mu(T)$ data appears fruitless because there are too many free parameters to obtain a unique result from the fit procedure. However, the mobility data taken over a wide temperature range are a valuable indicator regarding impurity contaminations and crystal perfection.

The free-electron concentration $n(1/T)$ of three SiC samples (#16, #17, #18) of different polytypes (3C, 4H, 6H) is plotted in fig. 3. The fitting procedure results in one (3C) and two (4H, 6H) N-related donor species, respectively; the following parameters are obtained:

#16: $\Delta E_N = 28\,\text{meV}$,
$N_{comp} = 2 \times 10^{17}\,\text{cm}^{-3}$,
$N_N = 2.5 \times 10^{17}\,\text{cm}^{-3}$;
#17: $\Delta E_{N,1} = 45\,\text{meV}$, $\Delta E_{N,2} = 100\,\text{meV}$,
$N_{comp} = 3 \times 10^{16}\,\text{cm}^{-3}$,

$N_{N,1} = 1.5 \times 10^{17}\ cm^{-3}$,

$N_{N,2} = 1.5 \times 10^{17}\ cm^{-3}$;

#18: $\Delta E_{N,1} = 80$ meV, $\Delta E_{N,2} = 130$ meV,

$N_{comp} = 6 \times 10^{15}\ cm^{-3}$,

$N_{N,1} = 8 \times 10^{16}\ cm^{-3}$,

$N_{N,2} = 2 \times 10^{17}\ cm^{-3}$.

The concentration ratio of the two donor species in the 4H polytype is $N_{N,1} : N_{N,2} = 1:1$ in accordance with the number of cubic and hexagonal lattice sites. In analogy to the 6H polytype, we attribute the shallow level ($E_c - 45$ meV) to N donors residing at a substitutional site with a hexagonal environment (h site), while the deeper level ($E_c - 100$ meV) will then have to belong to N donors on lattice sites with cubic environments (k site); for comparison with optical data, see part II.

Published values of ionization energies of nitrogen donors in 3C-, 4H- and 6H-SiC polytypes are summarized in table 2(a) to (c). This table provides a comparison of ionization energies determined by Hall measurements and by optical methods (IR absorption, donor–acceptor-pair photoluminescence); for 3C-SiC, the binding energy of the nitrogen ground state obtained from the effective-mass approximation calculated after Faulkner [17] is given in the last column.

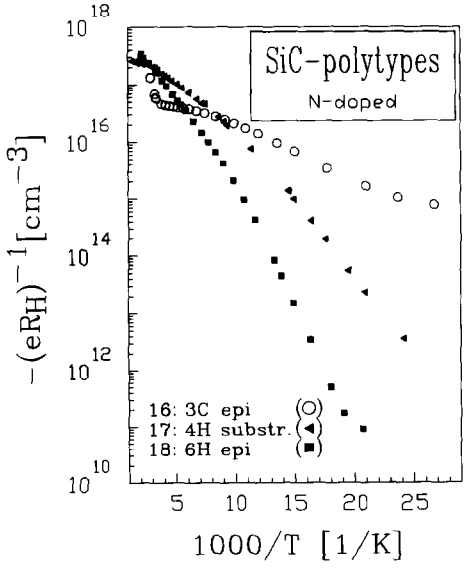

Fig. 3. Hall measurements on three SiC samples of different polytype (3C, 4H, 6H). Free-electron concentration as a function of the temperature. The impurity parameters are given in the text.

Table 2a
Comparison of ionization energies of the nitrogen donor in different SiC polytypes determined by Hall effect and by optical methods. For 3C-SiC, the EMA value calculated after Faulkner [17] is listed in the last column. (a) 3C-SiC; (b) 4H-SiC; (c) 6H-SiC.

3C	Ionization energies (meV)			
Lattice site	Hall effect		Optical methods DAP PL[b]	EMA[c] after ref. [17]
	Without correction	With correction[a] [21,23]		
Cubic (k)	18–37 [18,19,29,30,31]	48 [21,22]	53–55 [7,32,33,34]	47

Table 2b

4H	Ionization energies (meV)	
Lattice sites	Hall effect Without correction	Optical methods IR absorption
Hexagonal (h)	45 [8]	51.8 [8]
Cubic (k)	100 [8]	91.4 [8]

Table 2c

6H	Ionization energies (meV)		
Lattice sites	Hall effect Without correction		Optical methods IR absorption
	$N_N < 10^{18}\ cm^{-3}$	$N_N > 10^{18}\ cm^{-3}$	
Hexagonal (h)	84–100 [9,24,35]		81 [9]
Cubic (k_1)	125–150 [9,24,35]	70–92 [30,36,37]	137.6 [9]
Cubic (k_2)			142.4 [9]

[a] Correction according to $E_N(N_N) = E_N(0) - \alpha N_N^{1/3}$ (see ref. [21]).
[b] DAP PL = donor–acceptor pair photoluminescence.
[c] EMA = effective mass approximation.

Note the ionization energy of the N donor in highly compensated 3C-SiC samples determined by Hall effect (18–37 meV) is approximately one half the value (53–55 meV) determined by optical methods.

About this discrepancy there exist numerous viewpoints in the literature. W.E. Carlos et al. [20] examined carefully 3C-SiC films and correlated electron spin resonance (ESR) signals and photoluminescence (PL) with donor concentrations measured by the Hall effect. They conclude that neither PL nor ESR provide any evidence for the presence of a shallower donor than nitrogen. Segall et al. [21,22] adapted an empirical rule given by Pearson and Bardeen [23] to correct the nitrogen ionization energies for the impurity concentration. This rule considers the decrease in the ionization energy with increasing impurity concentration which probably results from a decrease in the average potential energy of an electron; this energy is inversely proportional to the average distance of separation between impurities, corresponding approximately to $N_D^{1/3}$ (see legend in table 2). Segall demonstrated that the electrically determined ionization energies corrected for the nitrogen donor concentration agree well with the optically determined ionization energies (see table 2(a)). We point out that Segall's arguments correctly account for the lowered Hall values in compensated samples.

In the case of 4H- and 6H-SiC, the situation is more complicated because of the two nitrogen-related levels that contribute to the slope of the $n(1/T)$-curve. As demonstrated in figs. 4(a) and (b) for a series of N-doped CVD-grown 6H films on 6H substrates, the slope becomes flatter with increasing nitrogen concentration [15]. From samples #21 to #25, the N concentration increases from $10^{16}\,\mathrm{cm}^{-3}$ to $3\times10^{19}\,\mathrm{cm}^{-3}$ which is correlated to an increasing N_2 flow during crystal growth. The $n(1/T)$-curves for samples #24 and #25 indicate impurity conduction for temperatures $T<200$ K (the free electron concentration is nearly independent of the temperature). The onset of an impurity conduction can also be observed by the steep increase of the low-temperature edge of the $\mu(T)$-curves. As a consequence, there is only a small temperature range left in the $n(1/T)$-curves appropriate for the fit procedure permitting only a rough estimate of the nitrogen level. A differentiation between donors residing at hexagonal and cubic lattice sites is no longer possible. The corresponding averaged ionization energies of the N donors are listed in table 2(c) in the column with $N>10^{18}\,\mathrm{cm}^{-3}$. A detailed Hall analysis of the ionization energy of the N donor in 6H-SiC was performed by Alekseenko et al. [24] taking into account the magnitude of the nitrogen concentration as well as the influence of the compensation.

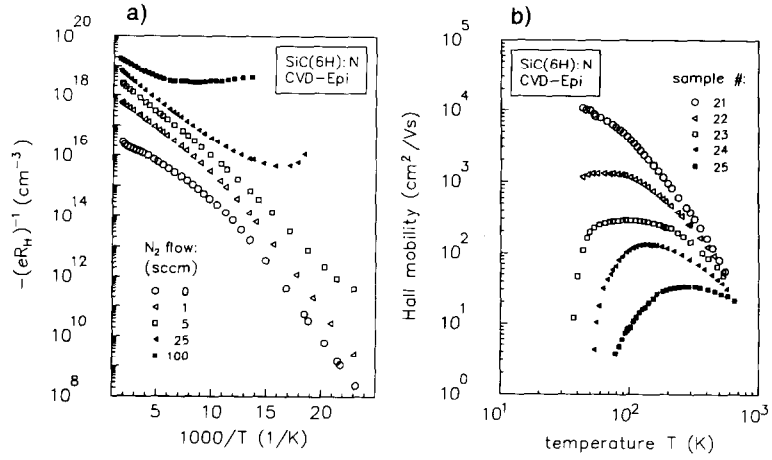

Fig. 4. Results of conductivity and Hall measurements of varying N-doped CVD-grown films. The nitrogen doping is achieved during the growth by variation of the N_2 flow. The impurity parameters are given in text.

1.2. Aluminum acceptor

For the analysis of Hall measurements in p-type SiC, we used the following hole parameters:
- hole density-of-states effective mass $m^*_{d,h} = m_0$ [25];
- spin degeneracy factor $g_i = 4$ (hexagonal polytypes);
- Hall scattering factor $r_H(T) = 1$.

From the fit of eq. (1) – modified for holes – to the temperature variation of the free hole concentration, we obtained an average value of 200 meV for the ionization energy of the Al acceptor in 6H-SiC. No dependence on inequivalent lattice sites is observed within the energy resolution of the Hall analysis. The same average value is obtained for the ionization energy of Al acceptors in 3C and 4H-SiC. These observations and the value of the Al ionization energy are in general agreement with the published data [26,27,28]. The scatter of published data ranges from 191 meV [26] to 280 meV [28]. At an Al concentration of 10^{18} cm^{-3}, we measured a maximum Hall mobility of 240 cm^2/V s at low temperatures ($\mu_p = 80$ cm^2/V s at room temperature). In contrast to donors it turns out that the ionization energy of acceptors in SiC is only weakly sensitive to a particular polytype and the different lattice sites (h or k).

1.3. Deep levels

The detection of deep levels in SiC is performed with a fast computer-controlled and fully automated deep-level transient spectroscopy (DLTS) system described in ref. [38]. The sensitivity of the system is increased by digital compensation of the sample capacitance and by averaging of a high number of transients. The trap parameters are determined during one temperature scan. The sample chamber permits temperature scans between 77 and 750 K. This temperature variation makes it possible to thermally emit charge carriers from deep levels that are separated up to approximately 1 eV from the band edges. For the DLTS measurements, Ti/Al Schottky contacts were prepared on the $(0\,0\,0\,\bar{1})$ C face of p/n-type SiC samples.

1.4. Boron-related centers

B^+ ions were implanted with various energies (20–100 keV) and doses (10^{11}–10^{13} cm^{-2}) at room temperature into Al-doped 6H-SiC epilayers. The implanted samples were heat-treated at temperatures of 1000°C to 1500°C for 2 to 4 min to remove the implantation damage and to electrically activate the boron atoms. DLTS investigations on such samples reveal two sharp peaks termed B and D as demonstrated in fig. 5. The D-level is also observed by admittance spectroscopy. A detailed discussion of these investigations is given in ref. [39]; some of the results are briefly reviewed here. From an Arrhenius analysis, we obtain the following ionization energies:

$\Delta E_B = 300$ meV,

$\Delta E_D = 580$ meV (see table 3).

Furthermore, the B- and D-level is found in 6H-SiC epilayers grown from the liquid phase and doped with boron during growth. Our investigations establish the B-level to be associated with the isolated boron acceptor.

The D-level can be generated in B-implanted samples at annealing temperatures above

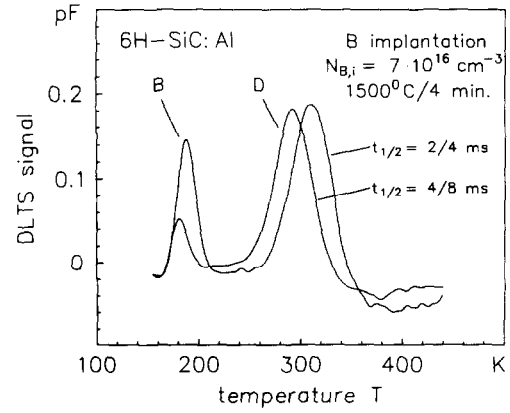

Fig. 5. DLTS spectra of a boron-implanted and annealed 6H-SiC sample for two rate windows: $t_1/t_2 = 2/4$ and 4/8 ms. The two peaks labelled B and D are due to the isolated boron acceptor and to the D-center, respectively. For temperatures $T < 190$ K, the DLTS signal is strongly affected by the freeze-out of the shallow Al dopant.

1000°C; its concentration depends linearly on the implanted B dose at comparable annealing conditions. Double correlated DLTS investigations reveal that the D-level is donor-like; its chemical nature is still an open question. We suggest that the D-level is a complex consisting of one boron atom and one or more native-defects.

1.5. Native defects

The DLTS spectrum (solid line) shown in fig. 6 is representative of as-grown n-type modified Lely crystals. It consists of two overlapping peaks labelled Z_1 and Z_2 [35,40]. A simulation program [35] was developed to determine the trap parameters from a least-squares fit to the experimental DLTS data; the evaluated peaks are indicated in fig. 6 by dashed lines. The trap parameters obtained from the DLTS spectrum in fig. 6 are as follows:

$$\Delta E(Z_1) = 620 \pm 20\ \text{meV},$$
$$N(Z_1) = 2 \times 10^{16}\ \text{cm}^{-3},$$
$$\sigma(Z_1) = 5 \times 10^{-17}\ \text{cm}^2;$$
$$\Delta E(Z_2) = 640 \pm 20\ \text{meV},$$
$$N(Z_2) = 1 \times 10^{16}\ \text{cm}^{-3},$$
$$\sigma(Z_2) = 2 \times 10^{-17}\ \text{cm}^2.$$

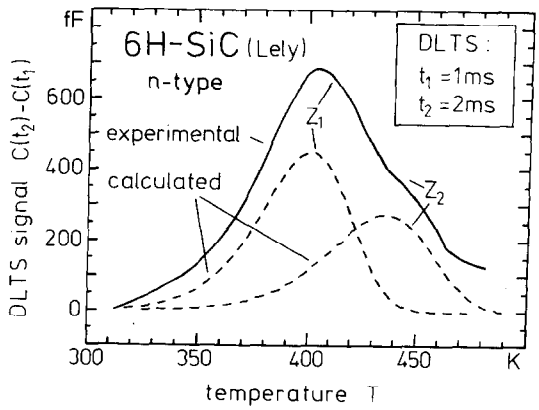

Fig. 6. DLTS spectrum taken on an as-grown n-type 6H-SiC sample. The solid curve represents the measured capacitance DLTS signal as a function of the temperature; the dashed lines are obtained from a least-squares fit to the experimental data. The trap parameters determined are given in the text.

Here $\sigma(Z)$ is the capture cross-section.

Z_1/Z_2 centers are homogeneously distributed in the bulk of the samples. Double-correlated DLTS investigations clearly indicate that the two centers are acceptor-like. They are not destroyed by heat treatments up to 1700°C. In n-type LPE-grown films of 6H-SiC, Z_1/Z_2-centers cannot be observed within the detection limit of $<10^{13}\ \text{cm}^{-3}$. However, Z_1/Z_2 centers can be generated in epilayers by either implantation of ions like Si, Ti, P, As, N, O or by irradiation of high-energy electrons ($E = 2$ MeV) with a fluence of $D = 9 \times 10^{15}\ \text{cm}^{-2}$ (see fig. 7). Vainer and Il'in [41] investigated 6H-SiC samples subsequent to a quenching process by photoinduced electron spin resonance (ESR) and identified an adjacent double vacancy (V_c–V_{Si}) showing C_{3v} symmetry. There are a series of correlations one can make of the generation and properties of Z_1/Z_2 acceptors and of the identified double vacancy. These common features may be a first indication that the Z_1/Z_2 acceptors and the double vacancy are identical. Because of their high thermal stability, Z_1/Z_2 centers may be of practical importance; they may be used to fabricate semi-insulating SiC substrates, in analogy to the EL2 center in GaAs.

Two further defects E_1/E_2 and E_3/E_4 are gen-

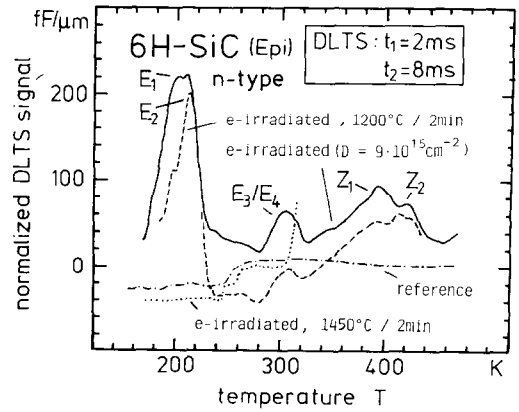

Fig. 7. DLTS spectra taken on n-type LPE-grown 6H-SiC films subsequent to different processing steps; the processing steps are indicated in the plot. The reference sample refers to the as-grown sample. All samples are cut from one wafer. Trap parameters of the defect centers observed in the e-irradiated film (without anneal) are given in table 3.

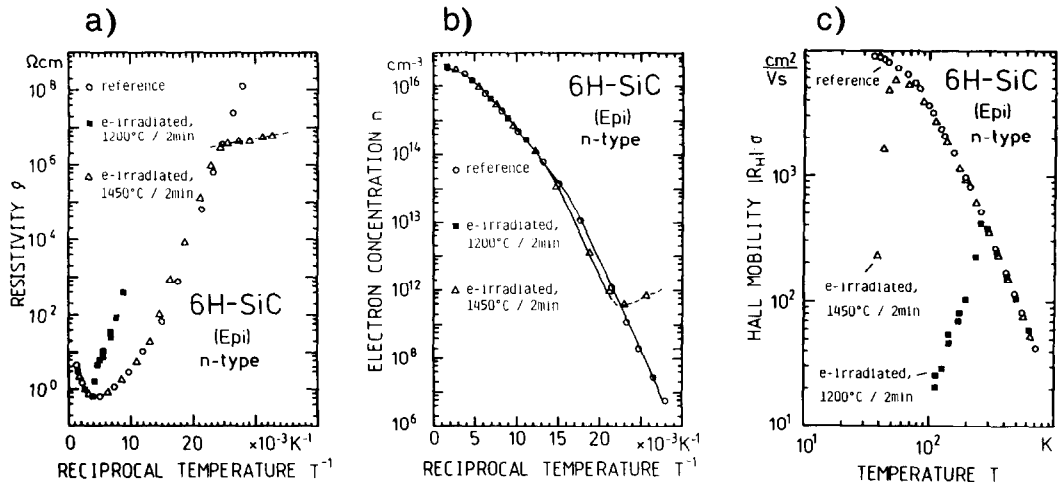

Fig. 8. Resistivity and Hall effect measurements of three differently processed 6H-SiC samples. The symbols represent experimental data. The samples were e-irradiated with a dose of 9×10^{15} cm^{-2}; the annealing conditions are given in the plots. The reference sample refers to the as-grown sample. (a) Resistivity vs reciprocal temperature; from the slope of the dashed straight line, an activation energy of 7 meV is determined. (b) Free-electron concentration vs reciprocal temperature; the solid lines are least-square fits to the measured points. (c) Electron mobility $\mu_H = \sigma R_H$ vs temperature.

Table 3
Boron-related impurities and native defects in SiC.

Level	Polytype	Energy position	Doping	Analysis method	Ref.
B	6H	E_V + 300 meV	Dur. growth	DLTS[a]/AS[b]	[39]
		E_V + 300 meV	Dur. growth	PL[c]	[44]
		E_V + 390 meV	Dur. growth	Hall effect	[45]
		E_V + 350 meV	Diffusion	DLTS[a]	[28]
		E_V + 400 meV	Diffusion	DAPL[d]	[46]
B-related	6H	E_V + 580 meV	Dur. growth/ implantation	DLTS[a]	[39]
(D-center)		E_V + 660 meV	Dur. growth	DLTS[a]	[28]
Native defects	6H				
Z_1		E_C − 620 meV (Acceptor)	Dur. growth/ e-irradiation	DLTS[a]	[35,40]
Z_2		E_C − 640 meV (Acceptor)	Dur. growth/ e-irradiation	DLTS[a]	[35,40]
E_1/E_2		E_C − 350 meV	e-irradiation	DLTS[a]	[35,40,42]
E_3/E_4		E_C − 570 meV	e-irradiation	DLTS[a]	[35,42]
		E_C − 600 meV	e-irradiation	DLTS[a]	[47]
		E_C − 1.1 eV	e-irradiation	DLTS[a]	[47]
		E_C − 130 meV	n-irradiation	Hall effect	[48]
		E_C − 240 meV	n-irradiation	Hall effect	[48]
		E_C − (0.5–0.9) eV	n-irradiation	Hall effect	[48]

[a] DLTS = deep level transient spectroscopy.
[b] AS = admittance spectroscopy.
[c] PL = photoluminescence.
[d] DAPL = donor–acceptor-photoluminescence.

erated by the e-irradiation as can be seen in fig. 7 [35,42]. Both peaks are composed of two overlapping peaks. It seems to be a general rule that in n-type 6H-SiC each defect species is generated in pairs with slightly differing ionization energies (possibly the generated defects reside at cubic and hexagonal lattice sites). The radiation-induced defects also affect the transport properties of the SiC material as demonstrated in fig. 8(a), (b) and (c). While the free-electron concentration $n(1/T)$ has not substantially changed, the resistivity $\rho(1/T)$ shows a steep increase for $T < 240$ K. Spatial fluctuations of the conduction band edge are assumed [43] to lead to a thermally activated mobility in the conduction band. The Hall mobility $\mu(T)$ strongly decreases for $T <$ 240 K. The radiation damage and the spatial fluctuations can partially be reduced by additional annealing steps (see open triangles in fig. 8). Published data on B-related impurities and native defects in 6H-SiC are summarized in table 3.

2. Optical characterization of SiC

From the early beginnings of the growth of SiC crystals by the Acheson technique (1893) optical and electro-optical measurements have played an important part in our developing an understanding of the physical phenomena observed in the polytypes of SiC. To mention but a few there is the pioneering goniometric investigation by B.W. Frazier [49] in 1893, the first measurements of the restrahlen bands in SiC by W.W. Coblentz [50,51] in 1906 and 1908 and the discovery and correct identification of light emission in a SiC diode by H.J. Round in 1907 [52]. Much of the material in the intervening years (1910–1989) has been reviewed several times [32,53–57] by one of the authors and the reader is referred to this material so that we can concentrate on reviewing some of the interesting developments since 1989. In part II of the paper we shall discuss the optical characterization of both SiC boule and SiC CVD epitaxial single-crystal film material which is representative of the state of the art in this field.

First we shall address the efficacy of applying low-temperature photoluminescence (LTPL) and low-temperature cathodoluminescence (LTCL) to the determination of polytypism, crystal and doping uniformity, the nature of shallow and deep impurities and optical signatures of point and line defects in SiC boule slices and SiC epitaxial films. We shall then discuss the use of Fourier transform infrared (FTIR) transmission to further elucidate the electronic level structure of the most prevalent donor, nitrogen, in 6H- and 4H-SiC [8,9]. Finally, we shall discuss the recently discovered [58] neutral four-particle acceptor complex in 3C-SiC and 6H-SiC. These Lampert complexes [59] are attributed to aluminum which is the most common acceptor in SiC.

2.1. Luminescence measurements

In our laboratories most photoluminescence experiments are carried out by immersing the sample in liquid helium pumped below the lambda point (2.172 K). Operating at 2 K avoids the noise generated by helium bubbles rising through the light path and it generally gives rise to sharp spectra. Sample temperatures from 4.2 to 300 K may be obtained in dewars with cold fingers or cooling the sample with He exchange gas at the desired conditions. Optical pumping is most often obtained with HeCd or Krypton lasers both of which have strong emission in the ultra-violet, well above the band gap of all the polytypes of SiC. For fast surveying a fast Fastie photographic spectrometer may be used. For normal analysis a standard Czerny–Turner monochromator with a cooled extended range photomultiplier (PMT) serves very well. One may use lock-in detection for bright samples or photon counting for weaker samples. Data acquisition and the control of the experiment is normally done by interfacing with a dedicated PC. For high-resolution experiments a grating two-meter stigmatic spectrometer is employed. For small selected regions of the spectrum the detection may be accomplished by use of a cooled CCD array. However, at the present time these arrays are still very expensive and cover only a minute part of the spectrum. The use of

specially sensitized ten-inch photographic plates is still a very effective means of obtaining high-resolution data. Here one has parallel processing over a large focal plane and the data is conveniently stored in a permanent record. The data is read out by a digitized microdensitometer which is tied to a dedicated PC. For Zeeman spectroscopy a split superconducting coil is used which will operate up to seven tesla while the sample is immersed in a separate cryostat which has variable temperature control. For uniaxial stress measurements a mechanical or gas-controlled piston device compatible with low-temperature operation is employed. In all these measurements care is taken that accurate polarization ratios may be obtained. Wavelength calibration is accomplished by superimposing spectral markers due to well-known noble gas discharge lines. An unknown line's position is determined by interpolation between two standard lines. This method is far more reliable than an overall calibration of the monochromator or spectrometer. We must always remember that all the polytypes of SiC are *indirect* semiconductors and as such the absorption of light near the bandgap is *weak*. Should we want to examine thin (<1 μm) epitaxial films of SiC the normally available pumping laser radiation is at a wavelength where very little of the energy will be absorbed in such thin films. Worse yet, if the films are grown on boule SiC this presents a serious problem of substrate interference for samples as thick as 5 μm. The solution is to use a soft (low-energy) electron beam as the exciting agent. However, since the SiC film must be at helium temperatures for best evaluation any condensation on the sample during the experiment must be avoided. The penetration of low-energy electron beams can easily be stopped by an accumulation of condensed gases in an apparatus with a modest vacuum. To this end we have built an ultra-high-vacuum, low-temperature cathodoluminescence (LTCL) spectrometer [60] which attains helium temperatures at a pressure of 10^{-11} Torr. This instrument can be loaded with six samples at one time but the preparation and out-gassing procedures are very time-consuming. Excellent results have been obtained with this instrument but it should be emphasized that there can be differences between the photoluminescence and the cathodoluminescence measurements and that magneto-optic experiments are impossible.

LTPL and LTCL are found to be very useful, nondestructive, diagnostic techniques for the determination of the nature and uniformity of polytype growth in SiC films and boule slices. In addition, much can be learned from these studies about shallow and deep centers introduced purposely or accidentally during the growth process. The best way to get a feeling for the power of LTPL or LTCL is to 'walk through' two spectra that compare SiC epitaxial films grown under substantially different conditions. In figs. 9 and 10 we compare the spectrum of an n-type CVD epitaxial film of 6H-SiC grown on the carbon face of a 6H-SiC single-crystal boule slice with the spectrum of a slightly p-type CVD epitaxial film of 6H-SiC grown on the Si face of a 6H-SiC single crystal boule slice. In fig. 9 both samples show the three non-phonon lines P_0, R_0, S_0 so characteristic of nitrogen-doped 6H-SiC. The three non-phonon lines are the recombination radiation of an exciton in a four-particle neutral donor complex at the three inequivalent donor sites of the 6H-SiC unit cell. However, when one compares the C-face growth with the Si-face growth differences are immediately apparent. In the C-face film the strong features below the non-phonon lines are primarily the phonon replicas of the P center. This is indicative of substantial nitrogen doping. However, in the Si-face spectrum we see three different features marked 4A, I and A_0. The 4A feature has now been attributed to an acceptor four-particle neutral complex and will be discussed in detail later. The series of lines marked I_{44}, I_{46}, I_{77}, I_{95}, I_{104} and I_{107} represent the radiative recombination of the intrinsic exciton in 6H-SiC with the emission of a momentum-conserving phonon whose energy in meV is given as a subscript. At low doping levels the ratio of the I_{77} intrinsic line to the three nitrogen non-phonon lines, or other non-phonon lines due to additional impurities, is an excellent indication of concentration of such impurities. One might ask how sensitive such a measurement is to the sample temperature. The inten-

sities of the *bound* excitons in SiC have been known not to vary very much between 1.3 and 2.1 K but until now not very much has been known about the *intrinsic* excitons. We have carried out a series of experiments which give the ratio of the intrinsic phonon replica I_{77} to the three P_0, R_0, S_0 non-phonon lines in 6H-SiC at temperatures varying from 1.3 to 2.14 K. The results are shown in table 4. It appears that the magnitude of the intrinsic exciton replica I_{77} does not change within the experimental uncertainties in this temperature range. We conclude that taking the ratios of features in the spectrum to the I_{77} line is not sensitive to temperature in this range and is a good indicator of concentration. One final feature on the Si-face spectrum is the A_0 line near 4333 Å. This non-phonon line is associated with Ti in 6H-SiC [32,61,62,63]. In fig. 10 we compare the spectra of the same two samples from 4300 to 4800 Å. In the C-face sample, prominent lines due to two phonon replicas of the P line and combinations of the P line phonon replicas and a center of the zone TO phonon, TO_Γ, are seen. On the other hand in the Si-face sample the non-phonon lines of the Ti center, A_0, B_0, C_0, and some of its phonon replicas are denoted. We have also marked a rather faint phonon combination line of the intrinsic exciton ($I_{77} + I_{95}$) just to indicate that such intrinsic lines can be seen. One can conclude that the Si-face sample, while representing state-of-the-art purity in present-day CVD SiC films, is far from being devoid of donors, acceptors or deep centers. Finally, these techniques may be used to study many other luminescent phenomena present in SiC crystals. One may study donor–acceptor pairs, impurity defect complexes and light emission from extended defects. In addition with the application of magnetic fields and stress on the crystals much can be learned about the detailed nature of shallow and deep centers in SiC. No laboratory that is presently engaged in SiC crystal or film growth should deny itself the obvious benefits of LTPL and LTCL diagnostics.

Table 4
Ratios of the intrinsic phonon replica I_{77} to the three nitrogen non-phonon lines of 6H-SiC (6H-SiC N-1484-1).

T (K)	1.3	1.8	1.91	2.01	2.14
I_{77}/S_0	1.3	1.2	1.2	1.2	1.2
I_{77}/R_0	1.75	1.65	1.72	1.66	1.70
I_{77}/P_0	23.9	25	23.7	21.3	24.4

2.2. *Nitrogen donors in 6H-SiC and 4H-SiC*

Another powerful optical technique, Fourier transform infrared (FTIR) absorption, has recently been used by Suttrop et al. [9] and Götz et al. [8] to study the details of the energy levels of the nitrogen donors in SiC with polytypes 6H and 4H. Both Lely platelets and boule slices were used for the 6H experiments whereas only boule slices were employed for the 4H work. Careful Hall measurements accompanied these absorption measurements and have already been described in the first part of this paper. The 6H-SiC samples used by Suttrop et al. [9] had various degrees of nitrogen doping and compensation. Several new absorption lines have been resolved in the infrared in the range of wave numbers 400–750 cm^{-1} and 1000–1250 cm^{-1}. Thermalization effects were studied from 7 to 80 K and the polarization properties of the absorption features was also noted. A new model for the three nitrogen donors in 6H-SiC is proposed based on the effective mass approximation [17,64] taking into account the anisotropy of the electron effective mass and the valley–orbit splitting of the ground state. We recall that the usual notation for the inequivalent sites in the polytypes of SiC are h for the hexagonal site and k for the cubic site. Hence in 6H-SiC we have one hexagonal site h and two cubic sites k_1 and k_2 whereas in polytype 4H we expect to have only one h and one k site. There is no space to show the many absorption spectra which are given in the original paper [8,9] and we shall just give the results of the analysis of the date.

(1) The ground state valley–orbit splitting for the h-inequivalent site is found to be 12.6 meV. This is in excellent agreement with the 13 meV found from Raman scattering in 6H-SiC [65].

(2) The effective mass approximation is found

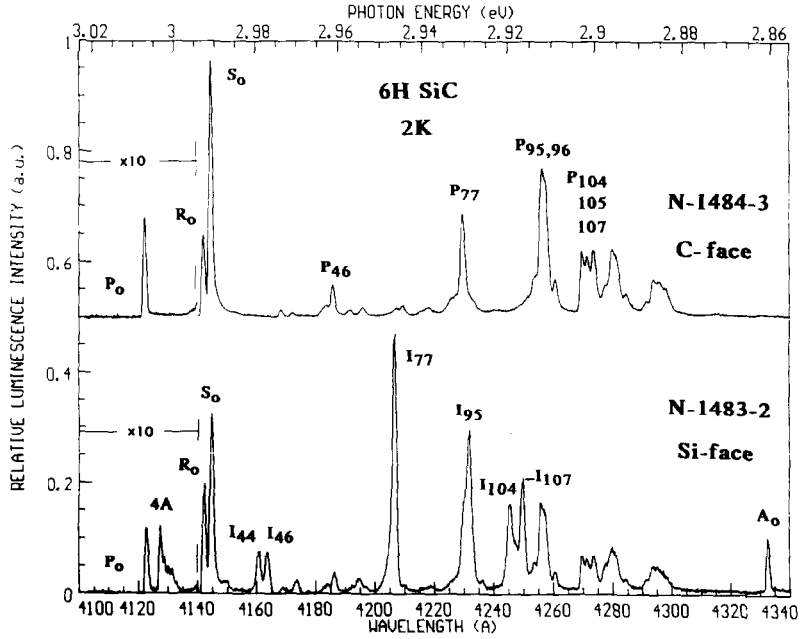

Fig. 9. A comparison of the low-temperature photoluminescence spectra of epitaxial films of 6H-SiC near the band edge. The single-crystal film N-1484-3 was grown on the carbon face of a 6H-SiC boule substrate whereas film N-1483-2 was grown on the Si face of a 6H-SiC boule substrate. Sample N-1484-3 was n-type whereas sample N-1483-2 was very slightly p-type.

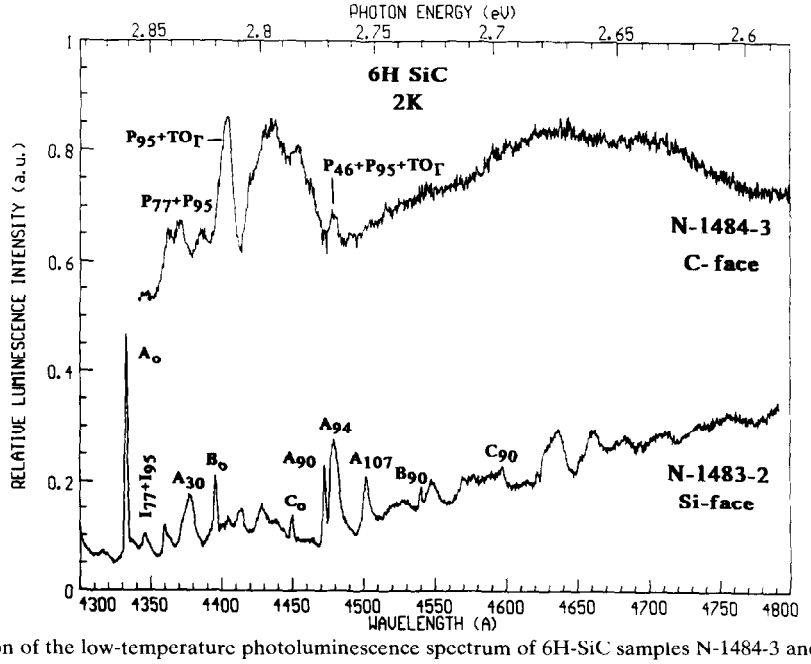

Fig. 10. A comparison of the low-temperature photoluminescence spectrum of 6H-SiC samples N-1484-3 and N-1483-2. In sample N-1484-3 we see the two and three phonon replicas of the non-phonon line P_0 associated with nitrogen in 6H-SiC. In sample N-1483-2 we see, primarily, the non-phonon lines and some of their replicas of the Ti center in 6H-SiC. Some of the minor features may be attributed to the two and three phonon replicas of the intrinsic exciton in 6H-SiC.

to hold adequately for the excited states $2p_0$, $2p_\pm$, $3p_0$ and $3p_\pm$.

(3) The perpendicular ($m_\perp$) and parallel ($m_\parallel$) effective electron masses were determined by a fit of the observed absorption data to the effective mass theory. The result for 6H-SiC is that $(m_\perp) = 0.24m_0$ and $(m_\parallel) = 0.34m_0$.

(4) The ionization energies for the h, k_1 and k_2 nitrogen donors in 6H-SiC are found to be 81.0, 137.6 and 142.4 meV, respectively. While the accuracy of the measured transitions is 0.02 meV the accuracy of the stated ionization energies depends critically on how applicable the effective mass theory is to this system.

(5) In fig. 11 we show the energy level scheme as proposed by Suttrop et al. [9] for the three inequivalent sites (h, k_1, k_2) of the nitrogen donor in 6H-SiC.

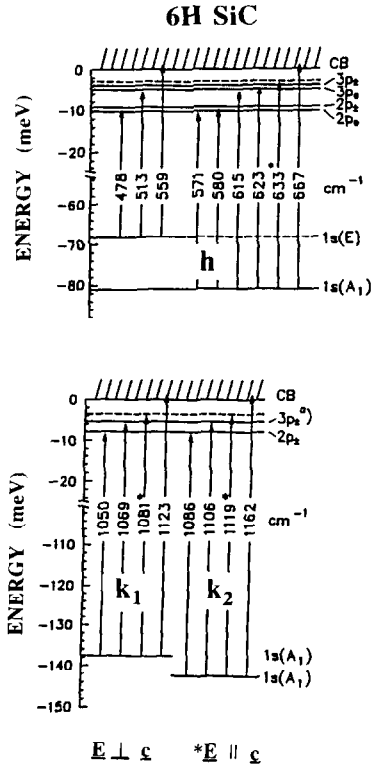

Fig. 11. The energy level scheme of the three nitrogen donors in 6H-SiC. The top of the figure gives the electronic transitions at the hexagonal site (h) of the 6H-SiC lattice. The bottom of the figure gives the electronic transitions at the two cubic sites (k_1, k_2) of the 6H-SiC lattice.

We now turn to the very recent results on nitrogen-doped 4H-SiC by Götz et al. [8]. Unfortunately the boule samples available thus far have only permitted examination of the spectra with the transmitting light entering the crystal along the c-axis ($\underline{E} \perp c$) and the crystal perfection of the available 4H material appears to be somewhat poorer than what is now commonly available for 6H-SiC. This situation will rapidly improve since several groups around the world are preparing to grow boule 4H-SiC. Nevertheless, important results have been achieved and they will now be discussed. As for the 6H samples, spectra were recorded in the range from 7 to 300 K but absorption lines are now found from 300 to 400 cm^{-1} and 680 to 740 cm^{-1}. By analogy with the 6H-SiC case it is assumed that the h inequivalent site in 4H-SiC also leads to the shallower of the two ground states. Hall measurements on these 4H-SiC samples have been made and have already been discussed in part I of this paper. The optical and Hall measurements are in reasonable agreement leading to a binding energy of 51.8 meV for the shallow state and 91.4 meV for the deeper state. This is completely consistent with the bound exciton binding energies in 4H-SiC of 7 and 20 meV. As in the case of the 6H-SiC absorption data, it appears that the 4H spectra can also be analyzed in the framework of the effective-mass theory and the valley–orbit splitting of the ground state. In addition to the ionization energies (51.8 and 91.4 meV) one obtains a perpendicular effective mass $(m_\perp) = 0.18m_0$ and a parallel effective mass $(m_\parallel) = 0.22m_0$. The valley–orbit splitting in the shallower level is found to be 7.3 meV in contrast to 12.6 meV in 6H-SiC. This is reasonable since the effective masses are found to be smaller in 4H-SiC. However, the experimental availability of the valley–orbit splittings in 6H-SiC and in 4H-SiC provides theorists with an unusual opportunity to test the importance of the central-cell correction and the effect of the Kohn–Luttinger interference effect [12] with the same atoms but in slightly altered non-nearest-neighbor environments.

2.3. An aluminum four-particle acceptor complex in 3C-SiC and 6H-SiC

As early as 1946 Busch and Labhart [66] reported that hexagonal black single crystals of SiC were of a p-type nature. It was presumably known at that time that such black crystals from large Acheson furnaces were heavily doped with aluminum and that therefore aluminum acted as an acceptor in SiC. A decade later Lely and Kröger [67] showed transmission curves from 0.3 to 10 μm of aluminum-doped (10^{19} cm^{-3}) hexagonal single crystals of SiC. Many attempts were made in the intervening years to study the aluminum acceptor by exciton spectroscopy but there was little success. Recently, Clemen et al. [58] have observed shallow and sharp emission lines in both 3C-SiC and 6H-SiC which was lightly doped with aluminum. They have associated this recombination radiation with an *acceptor* four-particle complex. Bogdanov and Gubanov [68] reported lines in the same spectral region from 6H-SiC platelets but interpreted these lines to be radiative recombination of a many-exciton impurity complex. Haberstroh [69] has also found similar lines, on rare occasions, in p-type 6H-SiC boule material grown at the Siemens Research Laboratories. Clemen et al. [58] used very high-resolution, low-temperature (1.3 to 2 K) photoluminescence and magneto-optics to examine these new lines. The samples were excited with a He–Cd laser which at 3250 Å has a ratio $I/I_0 = e^{-1}$ for a depth of ~1.5 μm for 3C-SiC [70] and ~4.0 μm for 6H-SiC [71]. Since most of the samples examined were CVD-grown epitaxial films on boule slices of 6H-SiC one has to be careful to avoid interference from the substrate. A 10 μm thick film of either 3C-SiC or 6H-SiC will avoid any such problem. Alternatively, the use of a laser further on in the ultraviolet will also permit the use of thinner films. For very thin films (<1 μm) low-temperature, low-voltage cathodoluminescence (LTCL) solves the problem but does not allow the use of magnetic fields for Zeeman spectroscopy. The samples used by Clemen et al. [58] were single crystal epitaxial films of 3C-SiC and 6H-SiC grown by chemical vapor deposition (CVD) at the NASA Lewis Research Center on 6H-SiC substrates or 6H-SiC films grown by Cree Research on 6H-SiC substrates. A trace of trimethyl aluminum (TMA) was added during growth to obtain the p-type films. No reliable concentrations for the aluminum are available but these lines have now been observed in many samples over a net concentration range of p-type dopant of about 10^{15} cm^{-3} to 4.0×10^{16} cm^{-3}. Figure 12 shows a LTPL spectrum of an 8 μm thick cubic (3C-) SiC (NASA 1324-5) film doped with TMA. We have marked the very familiar non-phonon line of the four-particle (4D) nitrogen neutral donor complex in 3C-SiC [72] as N_0 and its phonon replicas as TA, LA, TO and LO. In the background, one can see a contribution from the nitrogen–aluminum donor–acceptor pair (DAP) [73] spectrum marked by the numbers 4, 5, 7 and 8. The new feature, a four-particle acceptor complex at about 5250 Å, is marked 4A to be consistent with the four-particle donor complex notation. To date, phonon replicas of this 4A complex have not been identified and this may be due to the interference of the DAP lines [73]. The inset shows a more detailed LTCL spectrum of the 4A complex. At least five lines have been resolved at present and one expects to see more in the future as the sample preparation improves. As in GaP [74] the number of lines seen seems to be a function of the pumping intensity. It should be noted that the temperature of the LTCL spectrum is not exactly known at the moment but it is certainly above 4.2 K.

Figure 13 shows two spectra of a TMA-doped 6H-SiC film epitaxially grown on a 6H-SiC substrate at Cree Research. The three well-known non-phonon lines P_0, R_0, S_0 [75] of the four-particle nitrogen neutral donor complex are marked. In the top panel the 4A complex in 6H-SiC is seen between the P_0 and R_0 nitrogen non-phonon lines. It was obtained at 1.5 K at a resolution of 0.50 Å using photoelectric detection and a 3/4 meter Spex Czerny–Turner monochromator. The lower panel is obtained at a higher resolution of 0.1 Å on a two-meter, Baird-Atomic, stigmatic spectrometer using photographic plates. The plates are read on a

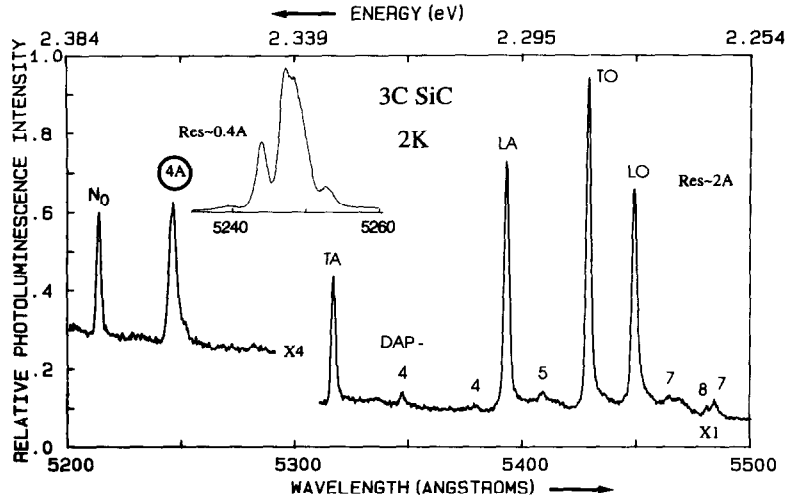

Fig. 12. The low-temperature photoluminescence spectrum N-1324-5. The top of the sample has an 8 μm thick single-crystal layer of cubic (3C-) SiC which was doped with aluminum by means of TMA. This layer was grown on top of a 4 μm undoped film of 3C-SiC which in turn was grown on the carbon face of a 6H-SiC wafer oriented 0.2° off the (0 0 0 1) plane. The inset shows part of a higher resolution scan of the low-temperature cathodoluminescence spectrum of this sample in the neighborhood of the four-particle neutral acceptor complex lines (4A). Five (4A) lines are resolved. The nitrogen (4D) non-phonon line and its phonon replicas are marked N_0, TA, LA, TO. Near-neighbor shell numbers of the nitrogen–aluminum donor–acceptor pair spectrum are denoted by the numerals 4, 5, 7 and 8.

Jarrel–Ash micro-densitometer and subsequently digitized. The main non-phonon lines of the 4A complex are labeled as l_1 and l_2. While the higher resolution gives a fine structure not seen in the top panel it fails to record some of the weaker lines seen at lower resolution with photoelectric detection. We believe that as many as twelve non-phonon lines may be attributed to this neutral acceptor complex. Presently, investigations are under way to study this structure under higher intensities with LTCL. Clemen et al. [58] have identified these new spectral features with the recombination of an exciton in an acceptor four-particle complex, involving aluminum which substitutes on the Si sublattice in SiC. If one is familiar with Haynes' rule as first applied to Si [76] this assertion would seem unreasonable. In a Haynes plot we have the exciton binding energy, E_{BX}, associated with the four-particle complex as the ordinate and the ionization energy E_D/E_A of the donor/acceptor on the abscissa. Haynes obtained a linear relationship between these two quantities in the case of Si for a variety of shallow impurities. In the case of Si, lines drawn through points obtained for the donors and acceptors nearly cross at the origin and the slope of the acceptor line is just somewhat smaller than that for the donor line. If Haynes' rule would have the same functional relationship in SiC as in Si we would *not* expect the deep aluminum acceptor in 3C-SiC (~250 meV) to have 4A lines only a factor of two deeper than the 4N line in 3C-SiC. On reflection one realizes that the Haynes rule pertaining to GaP is really a much better model for thinking about the situation in SiC. In GaP the intercept at zero binding energy is negative for donors and +3.5 meV for acceptors. In addition, the slope of the line representing the donors is about a factor of two larger than that for the acceptors. Thus for acceptors in GaP the exciton binding energy does not strongly depend on the ionization energy E_A. We are thus less surprised to find shallow spectral lines in cubic SiC and 6H-SiC that may be attributed to shallow 4A complexes.

Dean et al. [74] made use of group theory to argue that a large number of closely spaced lines is expected for the recombination of shallow 4A

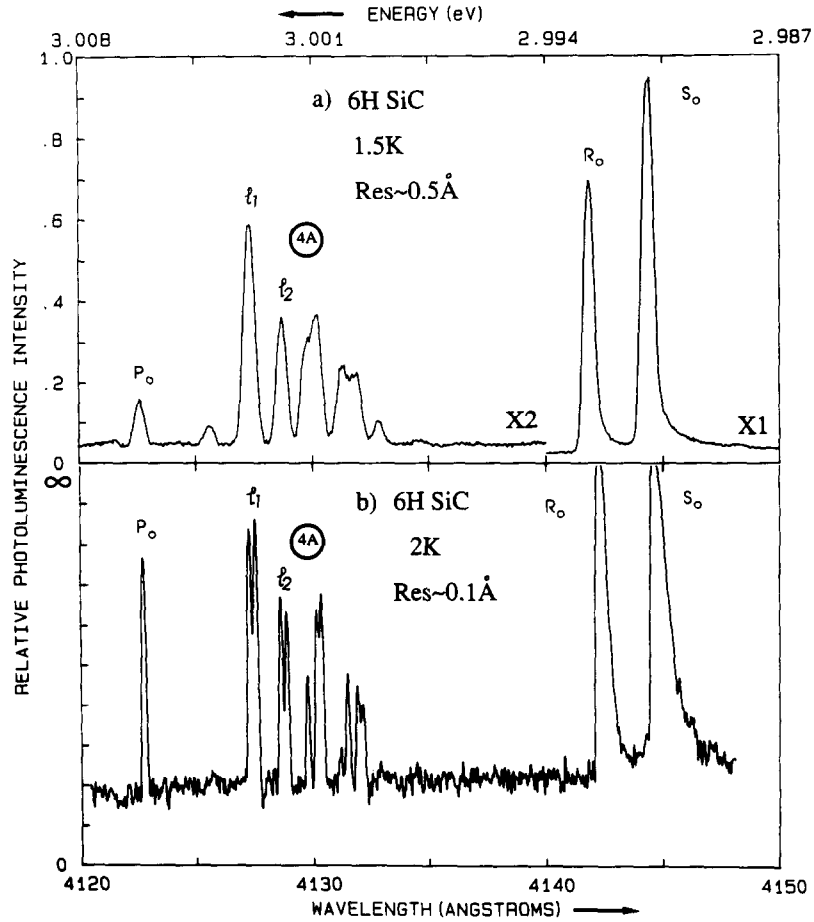

Fig. 13. Low-temperature photoluminescence spectra of C-B0270-8-np. The sample is a 3 μm thick lightly doped Al single-crystal film of 6H-SiC grown on an off-axis 6H-SiC boule substrate. Shown are the nitrogen (4D) non-phonon lines P_0, R_0, S_0 and the two strongest lines from the new (4A) complex marked I_1 and I_2. (a) Spectrum obtained using a photon counting system. (b) Spectrum obtained (at higher resolution) using photographic plates and one hour exposure time.

complexes in GaP (zincblende structure). Clemen et al. [58] applied this model to 3C-SiC which also has the zincblende structure and a similar band structure. Figure 14 illustrates the scheme which they developed for 3C-SiC. It is a schematic representation of the symmetry model for an acceptor four-particle complex at a *silicon* site with T_d symmetry in 3C-SiC. The diagrams indicate how two holes and an electron are combined to obtain a multiplet of closely spaced initial states of the four-particle complex. The degeneracies of the levels are shown in parentheses and the ordering of the levels is arbitrary. The final states of this system are not shown. They are the states of a neutral acceptor in its ground state. The single hole belongs to Γ_8 in T_d symmetry. The model predicts 12 distinct energy levels (ignoring accidental degeneracies) for the ground state multiplet of this 4A Lampert complex. To date only five lines have been seen but the model seems to be a plausible explanation for the complexity of the observed spectrum. A similar model was proposed to explain the multiplicity of transitions associated with the recombination of a four-particle acceptor complex in hexagonal 6H-SiC. Figure 15 gives the schematic representation of the symmetry model for this four-particle complex at a *silicon* site, with C_{3v}

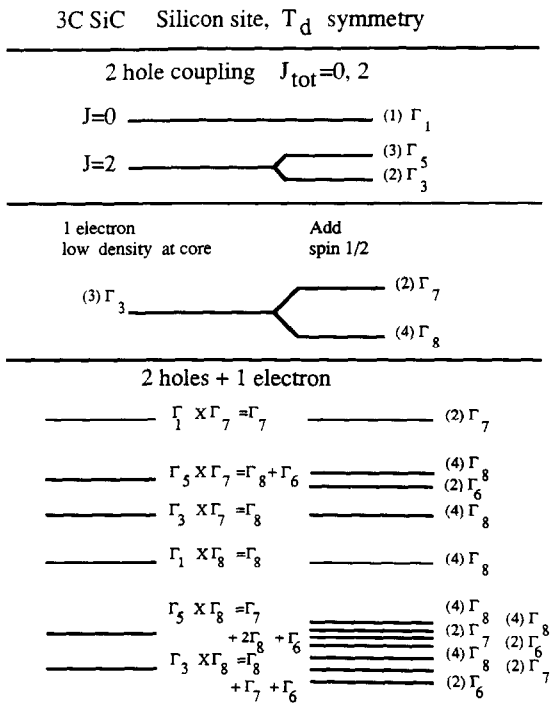

Fig. 14. Schematic representation of the symmetry model for an acceptor four-particle complex (4A) at a silicon site in cubic (3C-) SiC.

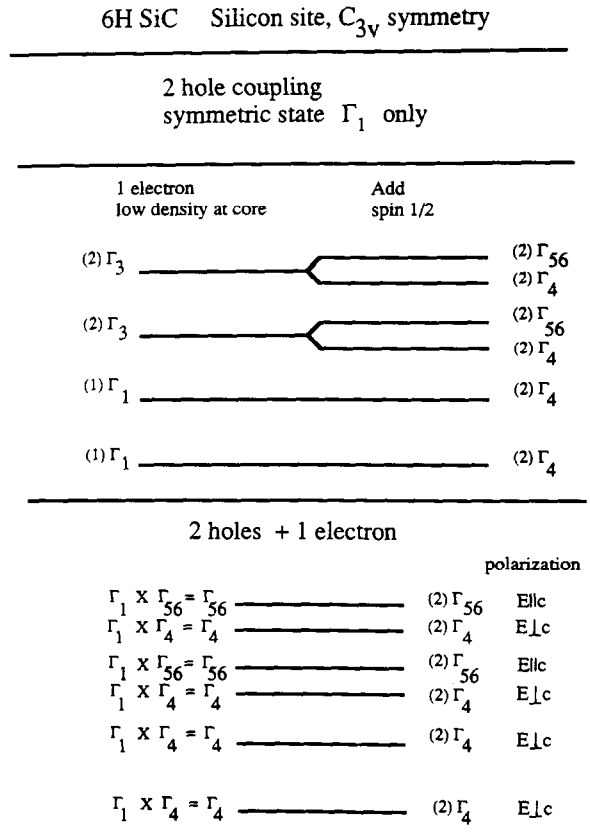

Fig. 15. Schematic representation of the symmetry model for an acceptor four-particle complex (4A) at a silicon site in hexagonal (6H-) SiC.

symmetry in 6H-SiC. As in fig. 14, the diagrams show how two holes and an electron are combined to obtain a multiplet of closely spaced initial states of the four-particle complex. As before, the degeneracies of the levels are shown in parentheses and the ordering of the levels is arbitrary. The final states are those of the neutral acceptor in its ground state. The single hole belongs to Γ_{56} in C_{3v} symmetry. When the singlet hole state with Γ_1 symmetry in C_{3v} is combined with the electron states of the 4A complex one obtains six doublets with symmetries $4\Gamma_4 + 2\Gamma_{56}$ for the initial states of the four-particle complex. The figure also shows the transitions allowed by symmetry with the electric field vector of the emitted radiation perpendicular or parallel to the symmetry axis. In principle we have three inequivalent sites for the acceptor in 6H-SiC so we should expect a maximum number of distinct energies for the initial states to be 3×6 or 18. At the present time one is unable to assign specific transitions but a model of the type given in ref. [58] seems able to account for the multiplicity of the observed transitions. It is likely that the observed lines both in 3C-SiC and in 6H-SiC can be attributed to radiative recombination of an acceptor four-particle Lampert complex. The experimental link to aluminum seems inescapable.

Acknowledgements

We should like to thank all our colleagues and students who have contributed so much to this study of SiC. Space permits us only to single out a few of the contributors who have done most to specifically address the issues in this contribution. We therefore should like to give special thanks to L.L. Clemen, R.P. Devaty, W. Götz, H.S. Kong, M.F. MacMillan, J.A. Powell, M.

Schadt, A. Schöner, W. Suttrop and M. Yoganathan for their steadfast efforts and contributions toward elucidating the physical properties of SiC discussed in this paper.

References

[1] Y.M. Tairov and V.F. Tsvetkov, J. Cryst. Growth 43 (1978) 209.
[2] S. Nishino, J.A. Powell and H.A. Will, Appl. Phys. Lett. 42 (1983) 460.
[3] W.F. Knippenberg, Phillips Res. Rep. 18 (1963) 161.
[4] G. Pensl, in: Landolt–Börnstein New Series III/22b, ed. M. Schulz (Springer-Verlag, Berlin, 1989) p. 51ff.
[5] R. Schaub, G. Pensl and M. Schulz, Appl. Phys. A 34 (1984) 215.
[6] R. Kaplan, R.J. Wagner, H.J. Kim and R.F. Davis, Solid State Commun. 55 (1985) 67.
[7] P.J. Dean, W.J. Choyke and L. Patrick, J. Lumin. 15 (1977) 299.
[8] W. Götz, A. Schöner, G. Pensl, W. Suttrop, W.J. Choyke, S. Leibenzeder and R. Stein, accepted at the 5th Int. Conf. on Shallow Impurities in Semiconductors, Kobe, Japan, 1992.
[9] W. Suttrop, G. Pensl, W.J. Choyke, R. Stein and S. Leibenzeder, J. Appl. Phys. 72 (1992) 3708.
[10] Y. Li and P.J. Lin-Chung, Phys. Rev. B 36 (1987) 1130.
[11] H.-G. Junginger and W. van Haeringen, Phys. Stat. Sol. 37 (1970) 709.
[12] L.A. Patrick, Phys. Rev. B 5 (1972) 2198.
[13] G. Ziegler, P. Lanig, D. Theis and C. Weyrich, IEEE Trans. Electron. Devices 30 (1983) 277.
[14] L. Hoffmann, G. Ziegler, D. Theis and C. Weyrich, J. Appl. Phys. 53 (1982) 6962.
[15] S. Karmann, W. Suttrop, A. Schöner, M. Schadt, C. Haberstroh, F. Engelbrecht, R. Helbig, G. Pensl, R.A. Stein and S. Leibenzeder, J. Appl. Phys. 72 (1992) 5437.
[16] L. Patrick, J. Appl. Phys. 38 (1967) 50.
[17] R.A. Faulkner, Phys. Rev. 184 (1969) 713.
[18] A. Suzuki, A. Uemoto, M. Shigeta, K. Furukawa and S. Nakajima, Appl. Phys. Lett. 49 (1986) 450.
[19] A. Suzuki, A. Uemoto, M. Shigeta, K. Furukawa and S. Nakajima, Appl. Phys. Lett. 50 (1987) 1534.
[20] W.E. Carlos, W.J. Moore, P.G. Siebenmann, J.A. Freitas Jr., R. Kaplan, S.G. Bishop, P.E.R. Nordquist Jr., M. Kong and R.F. Davis, Mat. Res. Soc. Symp. Proc. 97 (1987) 253.
[21] B. Segall, S.A. Alterovitz, E.J. Haugland and L.G. Matus, Appl. Phys. Lett. 49 (1986) 584.
[22] B. Segall, S.A. Alterovitz, E.J. Haugland and L.G. Matus, Appl. Phys. Lett. 50 (1987) 1533.
[23] G.L. Pearson and J. Bardeen, Phys. Rev. 75 (1949) 865.
[24] M.V. Alekseenko, A.G. Zabrodskii and M.P. Timofeev, Sov. Phys. Semicond. 21 (1987) 494.
[25] H.J. van Daal, W.F. Knippenberg and J-D. Wasscher, J. Phys. Chem. Solids 24 (1963) 109.
[26] M. Ikeda, H. Matsunami and T. Tanaka, Phys. Rev. B 22 (1980) 2842.
[27] G. Zanmarchi, J. Phys. Chem. Solids 29 (1968) 1727.
[28] M.H. Anikin, A.A. Lebedev, A.L. Syrkin and A.V. Suvorov, Sov. Phys. Semicond. 19 (1985) 69.
[29] M. Yamanaka, H. Daimon, E. Sakuma, S. Misawa and S. Yoshida, J. Appl. Phys. 61 (1987) 599.
[30] T. Tachnibana, H.S. Kong, Y.C. Wang and R.F. Davis, J. Appl. Phys. 67 (1990) 6375.
[31] L.S. Aivazova, S.N. Gorin, V.G. Sidyakin and I. Shvarts, Sov. Phys. Semicond. 11 (1977) 1069.
[32] W.J. Choyke and L. Patrick, in: Silicon Carbide, eds. R.C. Marshall, J.W. Faust Jr. and C.E. Ryan (University of South Carolina, Columbia, SC, 1974) p. 261.
[33] H. Kuwabara, S. Yamada and S. Tsunekawa, J. Lumin. 12–13 (1976) 531.
[34] J.A. Freitas Jr., S.G. Bishop, P.E.R. Nordquist Jr. and M.L. Gipe, Appl. Phys. Lett. 52 (1988) 1695.
[35] H. Zhang, PhD Thesis (1990), Erlangen.
[36] G. Pensl, R. Helbig, H. Zhang, G. Zielger and P. Lanig, Mat. Res. Soc. Symp. Proc. 97 (1987) 195.
[37] A. Rosengreen, Mat. Res. Bull. 4 (1968) 355.
[38] K. Hölzlein, G. Pensl, M. Schulz and P. Stolz, Rev. Sci. Instrum. 57 (1986) 1373.
[39] W. Suttrop, G. Pensl and P. Lanig, Appl. Phys. A 51 (1990) 231.
[40] H. Zhang, G. Pensl, A. Dörnen and S. Leibenzeder, Extended Abstracts 89-2 (1989) 699.
[41] V.S. Vainer and V.A. Il'in, Sov. Phys. Solid State 23 (1981) 2126.
[42] H. Zhang, G. Pensl, P. Glasow and S. Leibenzeder, Extended Abstracts 89-2 (1989) 714.
[43] T.H.H. Vuons and R.J. Nicholas, J. Phys. C 18 (1985) 4021.
[44] A. Addamiano, R.M. Potter and V. Ozarow, J. Electrochem. Soc. 110 (1963) 517.
[45] G.A. Lomakina, Sov. Phys. Solid State 7 (1965) 475.
[46] V.S. Ballandovich, G.N. Violina and Yu. M. Tairov, Sov. Phys. Semicond. 15 (1981) 283.
[47] V.S. Ballanovich and G.N. Violina, Cryst. Latt. Def. Amorph. Math. 13 (1987) 189.
[48] A.I. Veinger, A.A. Lepneva, G.A. Lomakina, E.N. Mokhov and V.I. Sokolov, Sov. Phys. Semicond. 18 (1984) 1256.
[49] B.W. Frazier, J. Franklin Inst. Oct. (1893) 287–289.
[50] W.W. Coblentz, Carnegie Institution of Washington, Part III and IV (1906) 96.
[51] W.W. Coblentz, Carnegie Institution of Washington, Part V, VI, VII, Carnegie Institution of Washington (1908) 36.
[52] H.J. Round, Electrical World (1907) 309.
[53] W.J. Choyke, Mat. Res. Bull. 4 (1969) 141.
[54] W.J. Choyke, Inst. Phys. Conf. Ser. (1977) 58.
[55] W.J. Choyke, in: XX Colloquium Spectroscopicum Internationale and 7th Int. Conf. on Atomic Spectroscopy, Praha, 1977, p. 385.

[56] W.J. Choyke, in: MRS Symposium Series Vol. 97 (MRS, Pittsburgh, PA, 1987) p. 207.
[57] W.J. Choyke, The Physics and Chemistry of Carbides, Nitrides and Borides, NATO ASI Series Vol. 185 (Kluwer, Dordrecht, 1990) p. 563.
[58] L.L. Clemen, W.J. Choyke, R.P. Devaty, J.A. Powell and H.S. Kong, to be published in: Amorphous and Crystalline SiC IV (Springer-Verlag, Berlin, 1992).
[59] M.A. Lampert, Phys. Rev. Lett. 1 (1958) 450.
[60] W.D. Partlow, J. Ruan, R.E. Witkowsky, W.J. Choyke and D.S. Knight, J. Appl. Phys. 67 (1990) 7019.
[61] L.A. Patrick and W.J. Choyke, Phys. Rev. B 10 (1974) 5091.
[62] A.W.C. van Kemenade and S.H. Hagen, Solid State Commun. 14 (1974) 1331.
[63] K.M. Lee, Le Si Dang, G.D. Watkins and W.J. Choyke, Phys. Rev. B 32 (1985) 2273.
[64] B. Gerlach and J. Pollmann, Phys. Stat. Sol. B 67 (1975) 93.
[65] P.J. Colwell and M.V. Klein, Phys. Rev. B 6 (1972) 498.
[66] G. Busch and H. Labhart, Helv. Phys. Acta 19 (1946) 463.
[67] J.A. Lely and F.A. Kröger, in: Semiconductors and Phosphors, eds. M. Schön and H. Welker (Interscience, New York, 1958) p. 514.
[68] S.V. Bogdanov and V.A. Gubanov, Fiz. Tekh. Poluprovodn. 22 (1988) 728 [Sov. Phys. Semicond. 22 (1988) 453].
[69] Ch. Haberstroh, private communication.
[70] W.J. Choyke, Z.C. Feng and J.A. Powell, J. Appl. Phys. 64 (1988) 3163.
[71] W.J. Choyke and L.A. Patrick, Phys. Rev. 172 (1968) 769.
[72] W.J. Choyke, D.R. Hamilton and L.A. Patrick, Phys. Rev. 133 (1964) A1163.
[73] W.J. Choyke and L.A. Patrick, Phys. Rev. B 2 (1970) 4959.
[74] P.J. Dean, R.A. Faulkner, S. Kimura and M. Ilegems, Phys. Rev. B 4 (1971) 1926.
[75] W.J. Choyke and L.A. Patrick, Phys. Rev. 127 (1962) 1868.
[76] J.R. Haynes, Phys. Rev. Lett. 4 (1960) 361.